

HIGHLY TRANSPARENT ZnO-SnO₂/PMMA UVC SHIELDING COATINGS WITH EXCEPTIONAL MECHANICAL STABILITY

NEVENA ČELIĆ¹, GORAN ŠTRBAC¹, IMRE GUT¹, NENAD TADIĆ², ONDREJ BOSAK³, SVETLANA LUKIĆ-PETROVIĆ¹

¹ Department of Physics, Faculty of Sciences, University of Novi Sad, Trg D. Obradovića 4, 21000 Novi Sad, Serbia

E-mails: nevena.celic@df.uns.ac.rs; grstrbac@uns.ac.rs; imre.gut@df.uns.ac.rs; svetlana@df.uns.ac.rs

² Faculty of Physics, University of Belgrade, Studentski Trg 12-16, 11000 Belgrade, Serbia

E-mail: nenad.tadic@ff.bg.uns.ac.rs

³ Institute of Materials, Faculty of Materials Science and Technology, Slovak University of Technology, Böttova 25, 917 24 Trnava, Slovak Republic

E-mail: ondrej.bosak@stuba.sk

Received May 17, 2023

Abstract. UV radiation can have a harmful effect on both humans and the environment. Therefore, developing UV shielding materials is an important step in protecting ourselves and the environment from the harmful effects of UV radiation. Here we present a detailed study of ZnO-SnO₂/PMMA nanocomposite coatings, which completely block UVC radiation. Additionally, we study the effect of the addition of ZnO-SnO₂ nanoparticles on mechanical properties in the means of Vickers microhardness and find out that they positively affect the microhardness of the PMMA coatings up to a certain concentration. Scanning Electron Microscopy (SEM) and Atomic Force Microscopy (AFM) reveal quite homogeneous distribution of nanoparticles for lower concentrations and the presence of nanoparticle aggregates for higher concentrations such as 1 wt.% and 5 wt.% of ZnO-SnO₂ nanoparticles.

Key words: ZnO-SnO₂ nanoparticles, UV shielding, polymer nanocomposite.

DOI: <https://doi.org/10.59277/RomJPhys.2023.68.620>

1. INTRODUCTION

In the last decades, the thinning of the ozone layer has led to an increase in the amount of UV radiation reaching the Earth's surface, which can cause numerous health problems. It can also have a negative impact on plant and animal life, as well as on the Earth's climate. UV radiation can even damage different materials, such as fabrics, plastics, and other materials used in construction. The radiation in the UVC range (100–290 nm) is much more harmful than UVB (290–320 nm) and UVA (320–400 nm) radiation [1]. Therefore, there is a growing need for developing effective UV shielding materials for different applications, including contact lenses, flexible displays and optical filters [2]. One approach to preparing UV-shielding

materials involves incorporating UV absorbing nanoparticles (NPs) or nanofillers into the polymer matrix [3].

Among different polymers, Polymethyl Methacrylate (PMMA), stood out due to its unique properties [4]. It is lightweight, flexible, has high scratch resistance, low cost and, most important, it is transparent to visible light over 92%, which in combination with UV absorbing NPs leads to potential UV shielding material [5]. Numerous researches have been conducted by adding wide bandgap NPs, such as ZnO, TiO₂, CuO and In₂O₃, into the polymer matrix, with an aim to develop novel materials with UV shielding properties [1–3, 6–8]. One of the challenges, when fabricating these materials, is to obtain a highly homogeneous distribution of NPs in the polymer matrix, which will not lead to the decrease in transparency due to a formation of aggregates.

Although developing highly efficient UV protecting coatings is of high importance, they are often exposed to challenging environmental conditions. Thus, manufacturing nanocomposite coatings with high mechanical stability is another concern for practical applications. Various factors affect the hardness of a polymer, including its molecular weight, degree of cross-linking, and the nature of the monomers from which it is formed. To improve their mechanical stability, different methods, such as thermal annealing and doping with inorganic NPs, are applied. It was shown that some kinds of nanofillers, such as graphene, Al₂O₃, ZrO₂, TiO₂, CaO and MgO, enhance the mechanical resistance of polymers [9–10]. Some of them could synergistically affect optical and mechanical properties making novel materials with UV blocking properties and improved mechanical stability.

Reinforcing polymer matrix with heterojunction ZnO-SnO₂ NPs, with a bandgap of ~ 3.04 eV, has led to materials with very high photocatalytic efficiency but, there is no evidence on preparation ZnO-SnO₂ polymer nanocomposite films for UV shielding applications [11].

In this paper, we report the preparation and characterization of highly homogeneous ZnO-SnO₂/PMMA nanocomposite coatings with high transparency in the visible range and blocking properties in the UVC region. The coatings were prepared utilizing a simple spin coating method with different NP concentrations. Along with optical measurements, we performed the evaluation of the mechanical properties of the coatings, by the means of an instrumented indentation method with an emphasis on the Vickers microhardness. With an aim to find the optimal preparation conditions, we investigate the influence of nanoparticle concentration in the PMMA matrix and its annealing temperature on the mechanical and optical properties of the coatings. In order to analyze the morphology of the samples and the distribution of NPs in the polymer matrix, ZnO/SnO₂-PMMA nanocomposite coatings were analyzed with the scanning electron microscope (SEM) and atomic force microscope (AFM).

2. MATERIALS AND METHODS

2.1. MATERIALS

All chemicals were used as received without purification. PMMA (molecular weight: 350000 Da, density: 1.188 g/ml, transition temperature: 105°C), in a powder form (0.2–1 mm in diameter), ZnO and SnO₂, both with a purity of 99.9 % and particle size $\leq 1 \mu\text{m}$ and Anisole ($\geq 99\%$ purity) were purchased from Sigma-Aldrich.

2.2. ZnO/SnO₂-PMMA NANOCOMPOSITE COATINGS PREPARATION

ZnO-SnO₂ NPs were prepared by a solid-state method, which is described previously [12]. PMMA was dissolved in anisole with a concentration of 100 mg/ml. The PMMA was left in anisole for five days until the complete dissolution. After the PMMA dissolution, different weight ratios of ZnO-SnO₂ NPs (0.1 wt.%, 0.5 wt.%, 1 wt.% and 5 wt.%) were dispersed in it using an ultrasonic bath. After 5 hours of sonication, four solutions with dispersed NPs in them and one pure PMMA solution were spin coated at 1000 rpm for 1 min on previously cleaned glass substrates. The pure solution was prepared as a reference sample. After spin coating, the samples were thermally annealed at 90°C, 115°C and 150°C.

2.3. CHARACTERIZATION OF THE ZnO/SnO₂-PMMA NANOCOMPOSITE COATINGS

The distribution of NPs and the morphology of the coatings were investigated using SEM-JEOL JSM 6460LV scanning electron microscope. Before the analyses, the gold film was sputtered on samples to make the surface conductive.

The topography and roughness of samples were characterized using an atomic force microscope (AFM; Veeco Instruments, model Dimension V). Micrographs were obtained in tapping mode under ambient conditions, using TAP300 tips (resonant frequency 300 kHz, force constant 40 N/m). Roughness data were obtained using diNanoScope software (version 7.0). Scan sizes were 5x5 μm .

The absorption spectra were recorded with Perkin Emler LAMBDA 950 UV-Vis-NIR spectrophotometer in the range of 250–800 nm. The measurements of mechanical properties were carried out on a Fischerscope HM2000 S system device with Vickers diamond indenter, calibrated according to the DIN EN ISO 14577-3 standard using a BK7 type reference block. The microhardness measurements were carried out on the surface of the coatings at room temperature under different applied loads from 20 – 400 mN at a constant loading time of the 40 s.

3. RESULTS AND DISCUSSION

3.1. MORPHOLOGY OF ZnO/SnO₂-PMMA NANOCOMPOSITE COATINGS

The investigated nanocomposite coatings were prepared by spin coating of pure PMMA solution and ZnO-SnO₂ dispersions in PMMA on glass substrates with NPs concentrations ranging from 0.1–5 wt.%. Prior to investigations of the optical and mechanical properties of the samples, we carried out the morphological characterization of the samples. Figure 1a, b, c and d shows the surface morphology of the nanocomposite coatings. The NPs are quite homogeneously distributed over the film with some tendency to form agglomerates for the loadings of 1 wt.% and 5 wt.%. The good dispersibility of the NPs in the polymer matrix is very important for the optical transparency of the coatings. The cross-section image of the same sample presented in Fig. 1e shows that the thickness of the coatings is $\sim 1 \mu\text{m}$.

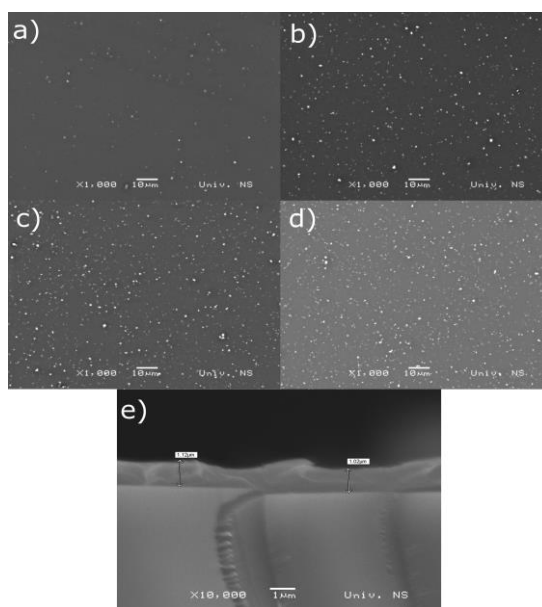


Fig. 1 – Surface morphology of ZnO-SnO₂/PMMA nanocomposite coating with: a) 0.1 wt.%; b) 0.5 wt.%; c) 1 wt.%; d) 5 wt.% ZnO-SnO₂ NPs; e) the cross-section image of the coating on the glass substrate.

In order to confirm the presence of aggregates in the samples with higher concentration of NPs, we performed AFM analyses on the sample with 5 wt.% ZnO-SnO₂ NPs. Figure 2 shows 2D and 3D $5 \times 5 \mu\text{m}$ topographic images of the ZnO-SnO₂/PMMA nanocomposite coating. It reveals that the NPs are homogeneously distributed over the sample surface, but the closer observation of the image discovers the presence of larger aggregates up to $\sim 500 \text{ nm}$ on the sample surface, which

agrees with presumptions based on SEM images (Fig. 1). The average roughness (R_a) of the coating is 12.5 nm.

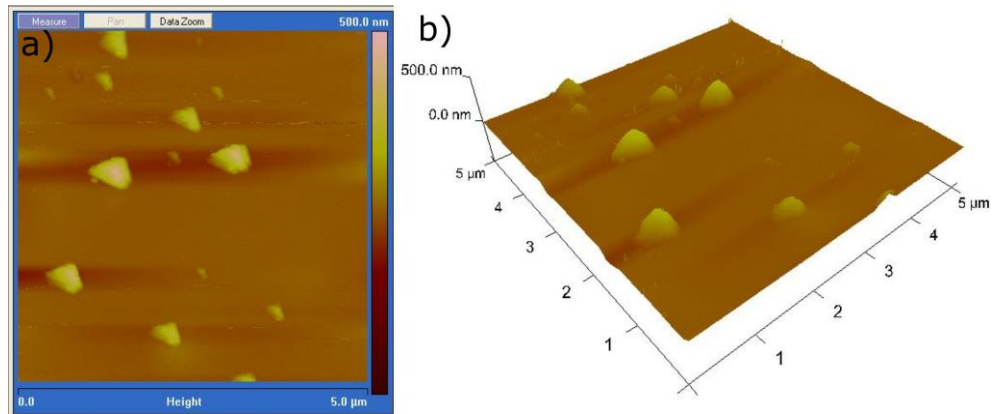


Fig. 2 – a) 2D and b) 3D AFM images of ZnO-SnO₂/PMMA nanocomposite coating with 5 wt.% of ZnO-SnO₂ NPs.

3.2. OPTICAL PROPERTIES OF ZnO-SnO₂-PMMA NANOCOMPOSITE COATINGS

The absorption and transmittance UV-Vis spectra of ZnO-SnO₂/PMMA nanocomposite coatings on glass substrate annealed at 150°C are presented in Fig. 3 and Fig. 4.

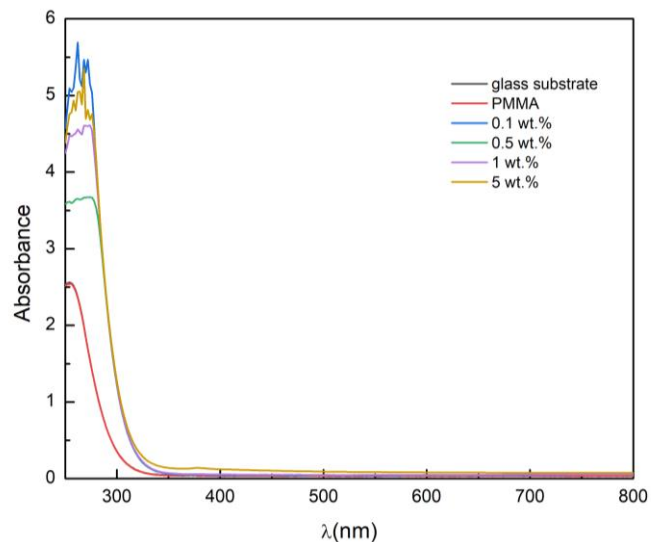


Fig. 3 – Absorption spectra of pure the glass substrate, pure PMMA and ZnO-SnO₂/PMMA nanocomposite coatings with different concentrations of ZnO-SnO₂ NPs.

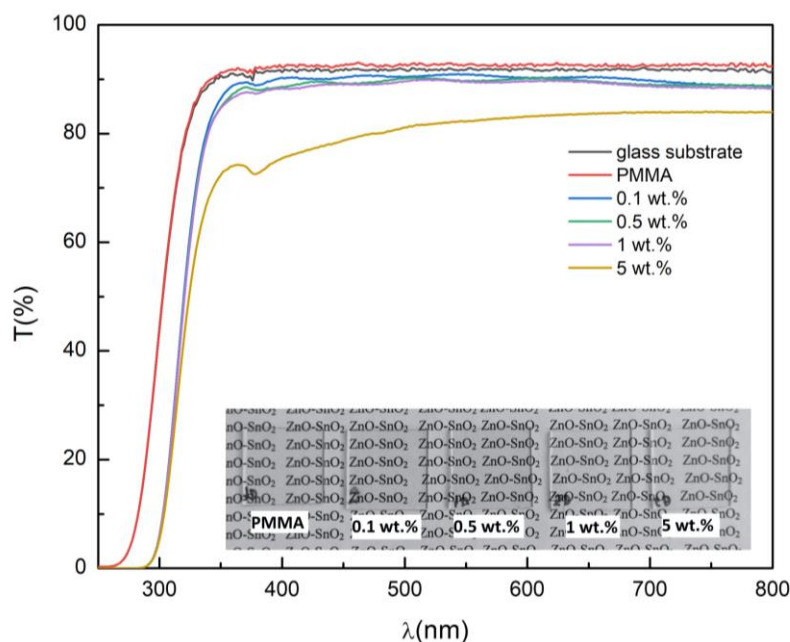


Fig. 4 – Transmittance spectra of pure the glass substrate, pure PMMA and ZnO-SnO₂/PMMA nanocomposite coatings with different concentrations of ZnO-SnO₂ NPs.

The nanocomposite films are transparent in the visible region, with transmittances similar to that of the pure PMMA film (~90%), except for the sample with 5 wt.% ZnO-SnO₂ NPs, which showed a larger decrease in transmittance for the visible wavelengths. This happens due to the formation of a larger amount of aggregates, which was confirmed by AFM (Fig. 2). It can be noticed that PMMA film on the glass substrate and the glass substrate by itself starts to absorb UV light at ~300 nm, while ZnO-SnO₂/PMMA nanocomposite coatings start to absorb at ~322 nm. The nanocomposite films containing only small concentrations of ZnO-SnO₂ NPs such as 0.1 wt.% show high UV blocking efficiency. On the other hand, all ZnO-SnO₂/PMMA nanocomposite coatings completely absorb UV light below 290 nm belonging to the UVC region (100–290 nm), which is very harmful to human health. The high transmittance of the coatings in the visible range can be attributed to the good dispersion of NPs in the PMMA matrix. An inset in Fig. 4 shows the photograph of the coatings proofing their high transparency. The negligible decrease in transparency can be noticed for the sample with 5 wt.% of NPs due to the formation of larger NP aggregates in the film, which was already confirmed from transmittance spectra.

The UV-Vis spectra presented in Fig. 5 show that annealing temperature has no effect on the transmittance of the coatings.

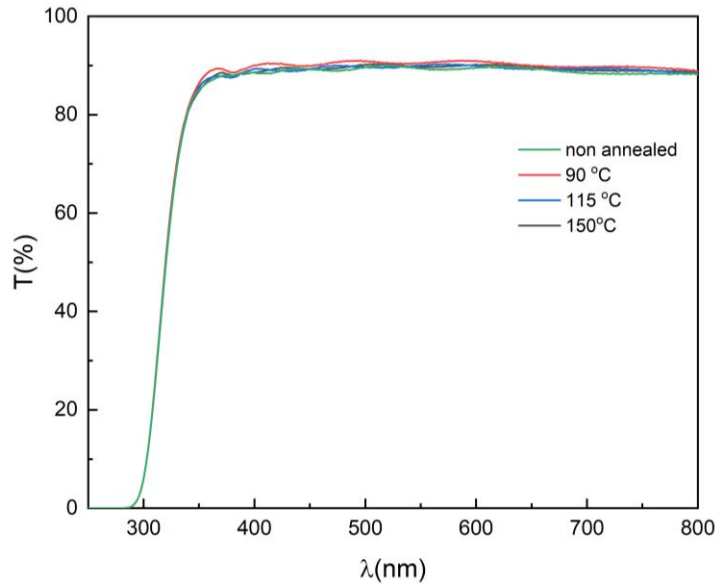


Fig. 5 – Transmittance spectra of ZnO-SnO₂/PMMA nanocomposite coatings with 0.5 wt.% of ZnO-SnO₂ NPs annealed at different temperatures.

3.3. MICROHARDNESS OF ZnO-SnO₂-PMMA NANOCOMPOSITE COATINGS

Figure 6 shows the dependence of Vickers microhardness on the applied load for pure PMMA and ZnO-SnO₂/PMMA nanocomposite coatings annealed at 150°C. The obtained values of microhardness $(2.5\text{--}3.3) \cdot 10^7$ Pa are comparable to those found in the literature for PMMA. It can be seen that the microhardness increases with the load for all samples, which is in agreement with the investigations of microhardness of PMMA published in the past [13]. The decrease of ZnO-SnO₂ NP concentration in the PMMA leads to the increase of Hv up to 0.5 wt.%, while for higher loadings Hv starts to decrease.

The dependence of microhardness on ZnO-SnO₂ NP concentration is presented in Fig. 7. The decrease of the microhardness for higher NP loadings can be explained by the formation of NP aggregates which change the polymer chain network in the proximity of the NPs.

The dependence of microhardness on annealing temperature shown in Fig. 8 suggests that microhardness increases with annealing temperature for all samples except for pure PMMA and the sample with 5 wt.% NPs, where it experiences drop at 150°C. Again, this different behavior in the sample with 5 wt.% could be attributed to the presence of aggregates in the PMMA matrix and weak ZnO-SnO₂/PMMA interaction [10, 14]. Additionally, the increase of microhardness with annealing suggests that the rearrangements of polymer chains and/or chemical reactions in it occur, which leads to the hardening of the PMMA [15].

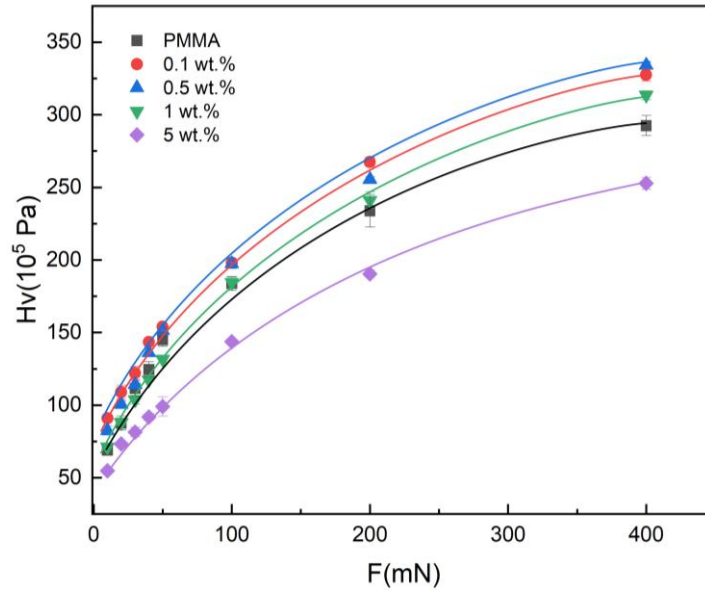


Fig. 6 – Variation of Vickers microhardness with applied load for pure PMMA and ZnO-SnO₂/PMMA nanocomposite coatings annealed at 150°C with different concentrations of ZnO-SnO₂ NPs.

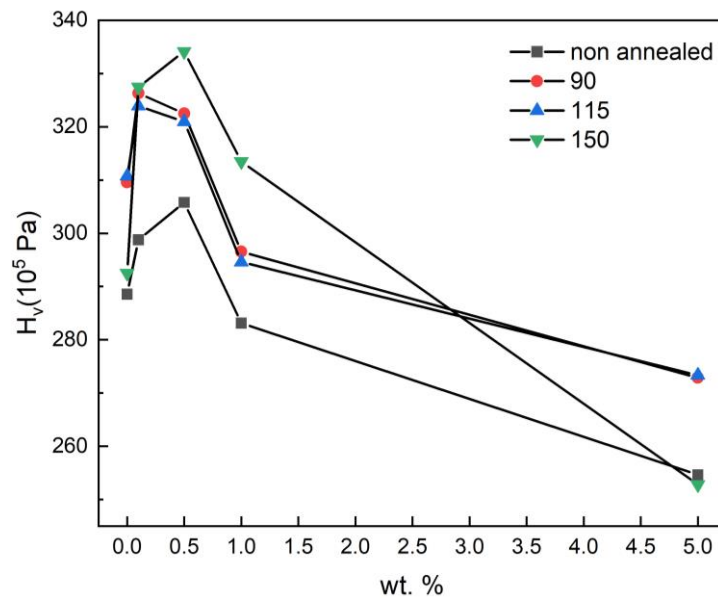


Fig. 7 – Variation of Vickers microhardness of ZnO-SnO₂/PMMA nanocomposite coatings with concentration of ZnO-SnO₂ NPs for load of 400 mN.

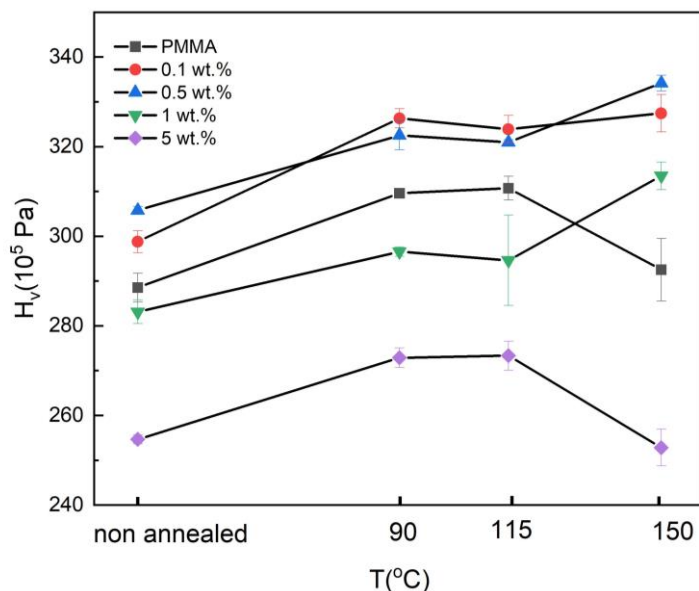


Fig. 8 – Variation of Vickers microhardness of ZnO-SnO₂/PMMA nanocomposite coatings annealing temperature for load of 400 mN.

Finally, the mechanical behavior of PMMA reinforced with ZnO-SnO₂ NPs is a complex interaction of the shape, distribution and amount of ZnO-SnO₂ NPs within the PMMA matrix, and the anisotropy they create [13]. Overall, the nanocomposite coating with 0.5 wt.% ZnO-SnO₂/PMMA annealed at 150°C showed the highest value of Vickers microhardness over all samples including the pure PMMA.

4. CONCLUSIONS

In this paper, we have presented a successful method for the preparation of ZnO-SnO₂/PMMA nanocomposite coatings which completely block UVC radiation and start to block in the UVB region with high transparency in the visible region. It was shown that complete blocking of UVC radiation appears for ZnO-SnO₂ NP concentrations as low as 0.1 wt.%. Reinforcing the PMMA matrix with ZnO-SnO₂ NPs not only improves optical properties, but also improves mechanical properties. Investigations of the influence of nanocomposite composition on Vickers microhardness reveals that it increases with ZnO-SnO₂ NP loading reaching a maximum at 0.5 wt.% and after that starts to decrease. Morphology and topography investigations confirm the presence of aggregates at higher NP concentrations, which probably deteriorate mechanical properties of the coatings. The examinations of the influence of annealing temperature on Vickers microhardness have shown that annealing has a positive

effect on microhardness, meaning that it increases with annealing temperature. Particularly, ZnO-SnO₂/PMMA coatings have the ability to completely absorb UV radiation of wavelengths smaller than 322 nm and have high mechanical resistance, which makes them perspective material for UV shielding applications.

Acknowledgments. The authors acknowledge the financial support of the Ministry of Education, Science and Technological Development of the Republic of Serbia (Grant No. 451-03-68/2022-14/200125) and the APV Provincial Secretariat for Higher Education and Scientific Research (Project: Novel chalcogenide materials for efficient transformation and use of energy, No.142-451-3128/2022-01/2).

REFERENCES

1. A. Gautam, A. Kshirsagar, S. Banerjee, V. Dhapte and P. Khanna, *J. Mater. Sci. Nanotechnol.* **4**, 1–14 (2016).
2. A. A. Ebnalwaled and A. M. Ismaiel, *Meas. J. Int. Meas. Confed.* **134**, 89–100 (2019).
3. J. Yang, J. Wang, M. Strømme and K. Welch, *J. Polym. Res.* **28**, 281 (2021).
4. A. Jaipean, P. Suriyakiat and K. Wasapinyokul, *AIP Conf. Proc.* **2010**, 020001 (2018).
5. L. N. Ismail, H. Zulkefle, S. H. Herman and M. Rusop Mahmood, *Adv. Mater. Sci. Eng.* **2012**, 1–6 (2012).
6. A. Singhal, K. A. Dubey, Y. K. Bhardwaj, D. Jain, S. Choudhury and A. K. Tyagi, *RSC Adv.* **3**, 20913–20921 (2013).
7. Y. Zhang, S. Zhuang, X. Xu and J. Hu, *Opt. Mater. (Amst).* **36**, 169–172 (2013).
8. Y. Zhang, X. Wang, Y. Liu, S. Song and D. Liu, *J. Mater. Chem.* **22**, 11971–11977 (2012).
9. M. Cierech, I. Osica, A. Kolenda, J. Wojnarowicz, D. Szmigiel, W. Łojkowski, K. Kurzydłowski, K. Ariga and E. Mierzwińska-Nastalska, *Nanomaterials* **8**, 305 (2018).
10. H. Wang, G. Xie, Z. Zhu, Z. Ying and Y. Zeng, *Compos. Part A Appl. Sci. Manuf.* **67**, 268–273 (2014).
11. N. Ćelić, N. Banić, I. Jagodić, R. Yatskiv, J. Vaniš, G. Štrbac, S. Lukić-Petrović, *ACS Appl. Polym. Mater.* **5**, 3792–3800 (2023).
12. T. B. Ivetic, B. Abramovic, M. Dimitrievska, G. Strbac, K. O. Čajko, B. B. Miljevic, L. R. Đaćanin and S. R. Lukić-Petrović, *Ceram. Int.* **42**, 3575–3583 (2016).
13. R. S. Jha, R. Bajpai and J. M. Keller, *IRJET* **3**, 1001–1004 (2016).
14. R. Sagar, M. S. Gaur, V. Kushwah, A. Rathore, D. G. Piliptsov and A. A. Rogachev, *Polym. Bull.* **78**, 7279–7300 (2021).
15. C. Man-Fang, Y. Fuqian and L. Sanboh, *Japanes J. Med. Instrum.* **75**, 161 (2005).